

A Comparative Study between Load and No-Load condition of Brushless DC Motor Drives by Using MATLAB

Upama Das^a, Pabitra Kumar Biswas^a, Sukanta Debnath^a

^aUpama Das, NIT Mizoram, Aizawl, India

Abstract

In this paper an extensive comparative performance study is carried out between No-load and load condition of an open loop model of a Brushless Direct Current (BLDC) Motor drive fed from a two-level voltage source inverter (VSI) under 120-degree conduction mode, using simulations in a MATLAB based software environment. BLDC motors are currently growing in popularity and replacing the brush motor in many applications, as they can be used in both low and high-speed vehicle systems and also in servo drives. The high reliability, torque to inertia ratio, high efficiency, high power density, ease of control and mainly the brushless operation make BLDC motors superior to others. It has a permanent magnet as a rotor with a balanced 3-phase armature in its stator. The armature winding is driven by a power electronics inverter which is switched in synchronism with the rotor position, sensed by an optical encoder or a Hall Effect sensor. It is found that torque ripple can be minimized by tuning the value of rotor position, no load condition and trapezoidal armature phase current. The different performance parameters for no-load and load condition of the BLDC motor such as phase voltages, phase currents, speed, electromagnetic torque, d and q axis current and rotor position etc. are determined in MATLAB environment.

Keywords: Brushless DC motor; Open loop model; voltage source inverter (120-degree mode); a position sensor (encoder); load and no load; MATLAB

1. Introduction

The Brushless DC motor is one type of Permanent Magnet Synchronous Machine (PMSM) where the stator is comprised of a balanced three-phase armature and the rotor is made of a permanent magnet. As the BLDC motor is a Synchronous motor, the stator and rotor field always operate at the same frequency, meaning there is no slip [1]. But unlike the Synchronous motor, BLDC motors have trapezoidal back emf. Basically, with the availability of permanent magnet materials and solid-state power semiconductors, conventional brushed DC motors led to the idea of developing BLDC motors [2]. A standard DC motor has multiple advantageous satisfying characteristics, such as good effectiveness, smooth speed control and linear torque-speed features. It has some disadvantages too, due to the presence of brushes. Reliability is limited at any time, operation can be hampered and the brushes may need replacing as they have a limited working life. Mainly, BLDC motors have been used to minimize this problem. This motor does not need any

extra DC supply like a conventional DC motor, as the flux is generated from a stable, permanent magnet rather than an electromagnet as in the case of a DC motor. Also, DC motors have poorer reliability compared to other motors, due to their use of carbon or metal brushes. This problem is solved by using electronic commutation and so the need of maintenance or replacement of brushes is no longer needed [3]. Thus the BLDC motor has a long operating life and higher speed range and is also designed with a compressed body. It is robust and enjoys high efficiency [4]. BLDC motors have some other advantages, such as high torque to inertia ratios, greater speed capabilities and better operational speed versus torque characteristics [5]. As mentioned earlier, BLDC motors are electrically commutated in a six step process; each step has two phases either positively or negatively energized, with one phase floating [6]. As the commutation of a BLDC motor is controlled electronically to rotate the BLDC motor, a specific sequence should be maintained to energize the stator windings. The information about the rotor position is important since the winding to be energized can be determined by the rotor position in the order of sequence. The rotor position is determined by what is basically a Hall effect sensor embedded into the stator [7]. In this paper, an open loop model for the BLDC motor is analyzed by

*Corresponding author

Email addresses: upama.eee@nitmz.ac.in (Upama Das),
pabitra.eee@nitmz.ac.in (Pabitra Kumar Biswas)

programming in MATLAB, considering the supply to the armature from a three phase two-level voltage source inverter (VSI) which operates under the 120° conduction mode of the inverter switches on the basis of the rotor position information. Brushless DC motor applications have been greatly accelerated in variable speed industrial drives by improvements in permanent magnet materials, in particular rare earth magnets. In open loop the speed control of such a machine can be carried out in a way similar to that of a conventional DC machine, by changing the equivalent conceptual “brush” position and varying the sensor position with respect to the rotor frame [5, 8].

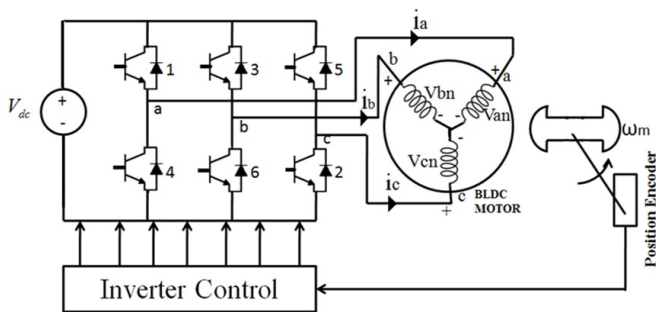


Figure 1: Schematic diagram of a BLDC motor fed from a two-level voltage source inverter

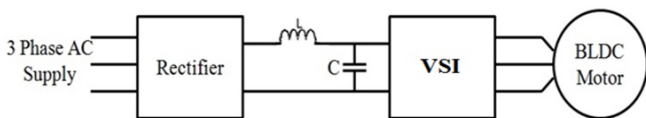


Figure 2: Overall open loop model of BLDC motor drive

Fig. 1 shows the drive system for which the proposed model is developed. The BLDC motor has three phase armature winding, with the three phase supply being given by a two-level voltage source bridge inverter which operates under the 120° mode of conduction. The inverter consists of six self-controlled switches viz. IGBTs with anti-parallel diodes. As mentioned earlier, the switching of the inverter devices is done in synchronism with the rotor position information. To gather rotor position information one sensor or transducer is placed on the rotor. Generally, a set of three infrared emitting diodes (IRED) and a gray-coded disc is required together with a corresponding set of three receptor photodiodes, placed on a stationary frame. This position sensor system generates three electrical pulses in digital form which are actually considered as a three-bit binary word; this bit value changes automatically after each 60° rotation of the rotor. Hence, the information on the rotor position is delivered after every 60° rotation [6]. Now, as the information is in binary form simple decoder logic is used to decode the information in order to provide the switching signals for the six self-controlled inverter devices, as per the 120° conduction logic. The inverter, in general terms, is a converter which converts a DC voltage to its equivalent AC voltage

as per requirements. Thus, here, a controllable DC voltage source, V_{dc} , which may be varied is connected to the inverter to achieve speed control in an open-loop configuration, as shown in Fig. 1. The same way armature voltage control is done in a conventional DC machine with a mechanical commutator to control the speed of the machine. The overall open loop model of the BLDC motor drive is shown in Fig. 2. The overall open loop model of BLDC motor drive consists of three main blocks, i.e. the voltage source inverter block, abc-dq transformation block and the BLDC motor, i.e. the machine block. This model of BLDC motor can be derived by assuming the inverter is to be operated in the 120° conduction mode [9–12].

3-Phase Voltage Source Inverter

Voltage source inverter, a DC voltage source with very small internal impedance, is used as input of the inverter. The DC side terminal voltage is constant, but the AC side output voltage may be constant or variable irrespective of load current. For one cycle of 360°, each step should be on a 60° interval for a six step inverter. In inverter terminology, a step is defined as a change in the firing from one switch to the next switch in proper sequence. There are two ways of gating the switch. One way is the 180° conduction mode, where each switch conducts for 180° and the other is the 120° mode of conduction, where each switch conducts for 120°. But in both these cases, gating signals are applied and removed at the same 60° intervals of the output voltage waveform [5]. Here, in the case of the BLDC motor, generally the 120° conduction mode is applied, as the voltage pattern is trapezoidal. Now, for the switching of a sequence of switches, the rotor position is monitored by an absolute position encoder and this encoded information is passed on to the controller block, which actually controls the operation of the inverter. This inverter controller block processes or decodes this information and from there generates the switching signals accordingly for the inverter [13, 14].

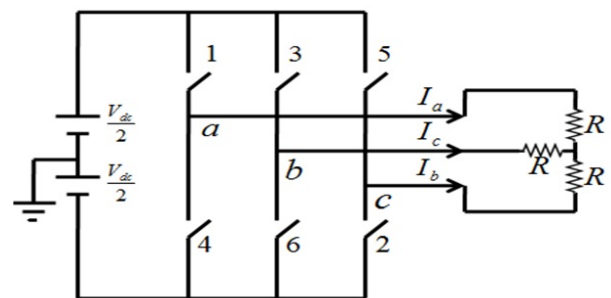


Figure 3: Schematic Diagram of Two level Three Phase VSI

There are some important points to be remembered in the case of the 120° conduction mode of inverter operation. One switch of the upper three inverter devices and one switch of the lower three inverter devices are always ON simultaneously. 120 Degree Conduction: There are six switching

Table 1: Phase Voltage of 120° mode of three phase VSI

Phase Voltage	61	12	23	34	45	56
V_{an}	$\frac{V_{dc}}{2}$	$\frac{V_{dc}}{2}$	0	$-\frac{V_{dc}}{2}$	$-\frac{V_{dc}}{2}$	0
V_{bn}	$-\frac{V_{dc}}{2}$	0	$\frac{V_{dc}}{2}$	$\frac{V_{dc}}{2}$	0	$-\frac{V_{dc}}{2}$
V_{cn}	0	$-\frac{V_{dc}}{2}$	$-\frac{V_{dc}}{2}$	0	$\frac{V_{dc}}{2}$	$\frac{V_{dc}}{2}$

sequences. Each SCR conducts for 120 degrees of a cycle. The switching sequence is 61, 12, 23,34,45,56. From Table 1 we can say that the total of the phase voltage is always nil and thus if one voltage is positive, another one is negative and the other phase voltage is nil. This is applicable for the whole switching sequence. As it is a 120 Degree Conduction mode two phases will always carry voltage and the other one will be of zero value[15–19].

Table 2: Line voltage of 120° mode of three Phase VSI

Line Voltage	61	12	23	34	45	56
V_{ab}	V_{dc}	$\frac{V_{dc}}{2}$	$-\frac{V_{dc}}{2}$	$-V_{dc}$	$-\frac{V_{dc}}{2}$	$\frac{V_{dc}}{2}$
V_{bc}	$-\frac{V_{dc}}{2}$	$\frac{V_{dc}}{2}$	V_{dc}	$\frac{V_{dc}}{2}$	$-\frac{V_{dc}}{2}$	$-V_{dc}$
V_{ca}	$-\frac{V_{dc}}{2}$	$-V_{dc}$	$-\frac{V_{dc}}{2}$	$\frac{V_{dc}}{2}$	V_{dc}	$\frac{V_{dc}}{2}$

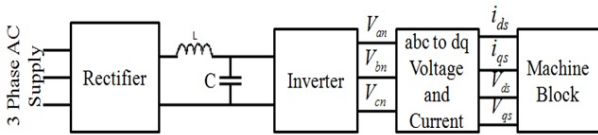


Figure 4: Block diagram of open loop model of BLDC motor drive system

2. The abc-dq Transformation Block

The BLDC motor with trapezoidal back EMF is analyzed using d-q reference frame theory [20]. The d-q reference frame theory is well-known, where a three-phase system (called a-b-c frame of reference) of current or voltage or flux linkage is transformed into an equivalent two phase system (called a d-q reference frame, actually d-q-0 frame, but zeroes sequence neglected, finally, assuming balanced operation) of current or voltage or flux linkage, by means of a transforming relationship, known as Park transformation. The slip ring to commutator transformation as introduced by Park transformation and others (a, b, c to d, q, 0) will now be considered. This is because the permanent magnet has distinct d and q axis. d-axis is taken along the axis of the PM flux and q-axis leads d-axis by 90°. Thus we may write

$$\begin{bmatrix} V_{d,q,0} \end{bmatrix} = K \begin{bmatrix} V_{a,b,c} \end{bmatrix} \quad (1)$$

then

$$\begin{bmatrix} i_{a,b,c} \end{bmatrix} = K^T \begin{bmatrix} i_{d,q,0} \end{bmatrix} \quad (2)$$

where

$$K = \begin{bmatrix} \cos\theta & \cos(\theta - 2\pi/3) & \cos(\theta + 2\pi/3) \\ -\sin\theta & -\sin(\theta - 2\pi/3) & -\sin(\theta + 2\pi/3) \\ \frac{1}{\sqrt{2}} & \frac{1}{\sqrt{2}} & \frac{1}{\sqrt{2}} \end{bmatrix} \quad (3)$$

$$\begin{bmatrix} v_d \\ v_q \\ v_0 \end{bmatrix} = \sqrt{\frac{2}{3}} \begin{bmatrix} \cos\theta & \cos(\theta - 120^\circ) & \cos(\theta + 120^\circ) \\ -\sin\theta & -\sin(\theta - 120^\circ) & -\sin(\theta + 120^\circ) \\ \frac{1}{\sqrt{2}} & \frac{1}{\sqrt{2}} & \frac{1}{\sqrt{2}} \end{bmatrix} \begin{bmatrix} v_a \\ v_b \\ v_c \end{bmatrix} \quad (4)$$

$$\begin{bmatrix} i_d \\ i_q \\ i_0 \end{bmatrix} = \sqrt{\frac{2}{3}} \begin{bmatrix} \cos\theta & \cos(\theta - 120^\circ) & \cos(\theta + 120^\circ) \\ -\sin\theta & -\sin(\theta - 120^\circ) & -\sin(\theta + 120^\circ) \\ \frac{1}{\sqrt{2}} & \frac{1}{\sqrt{2}} & \frac{1}{\sqrt{2}} \end{bmatrix} \begin{bmatrix} i_a \\ i_b \\ i_c \end{bmatrix} \quad (5)$$

Where θ is the angle between the d-axis of the rotor and q-axis at any instant of time. We may obtain v_d , v_q and v_0 as shown in equation 4 above, using voltage, current equation in the d-q axis reference frame. We can also find out the d-axis and q-axis current from equation (5) and also obtain the torque equation in the same reference [21–24].

3. The Machine

The mathematical modeling of BLDC motor is generally analyzed on the basis of “D-Q axes rotor reference frame theory” [25]. The ‘Machine’ block of the developed model accepts various components, such as the D-axis (V_{ds}) and Q-axis (V_{qs}) components of the BLDC motor stator (armature) voltage, the instantaneous rotor position value and the details of load torque (T_l , f_n) as inputs and calculates the other parameters viz. the stator currents and the flux linkages in stator in d-q frame and the electromagnetic torque (T_{em}). Next, the necessary equations related to the machine are shortened, with the symbols having their usual meanings [26–29]. The stator voltage and flux equation in the rotor reference frame are given below.

$$\psi_{qs}^r = L_q i_{qs}^r \quad (6)$$

$$\psi_{ds}^r = L_d i_{ds}^r + \psi_0^r \quad (7)$$

Where ψ_0 is the flux linkage due to the permanent magnet

$$v_{qs}^r = r_s i_{qs}^r + \omega_r \psi_{ds}^r + p \psi_{qs}^r \quad (8)$$

$$v_{ds}^r = r_s i_{ds}^r + \omega_r \psi_{qs}^r + p \psi_{ds}^r \quad (9)$$

The d and q axis voltage may be represented in a matrix form, which is given below

$$\begin{bmatrix} v_d \\ v_q \end{bmatrix} = \begin{bmatrix} r + L_{dq} & -\omega L_q \\ \omega L_d & r + L_{dq} \end{bmatrix} \begin{bmatrix} i_d \\ i_q \end{bmatrix} \quad (10)$$

$$\begin{aligned} T_{em} &= \frac{3}{2} \frac{P}{2} (\psi_{ds}^r i_{qs}^r - \psi_{qs}^r i_{ds}^r) \\ &= T_{em} = \frac{3}{2} \frac{P}{2} (\psi_{ds}^r i_{qs}^r - (L_d - L_q) i_{qs}^r i_{ds}^r) \end{aligned} \quad (11)$$

$$T_{em} = \frac{d\omega_m}{dt} + f_n \omega_m + T_l \quad (12)$$

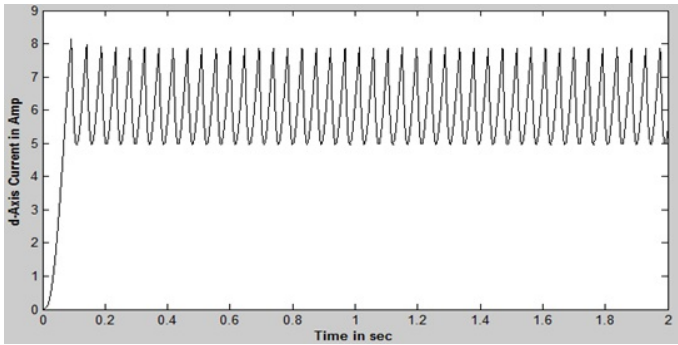


Figure 5: d-axis current vs. Time response of a BLDC Motor drive for $V_{dc}=48V$ and $T_I=0$

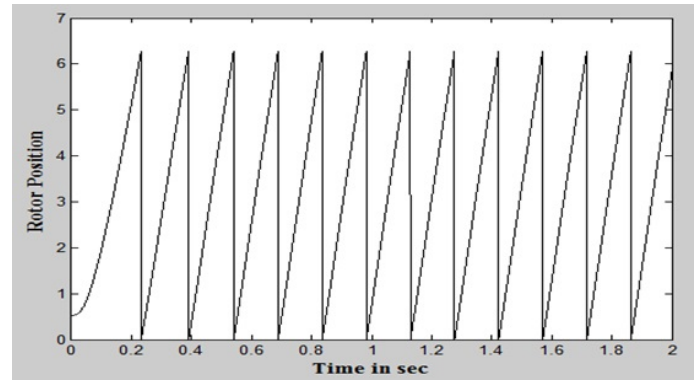


Figure 8: Rotor Position vs Time response of a BLDC Motor drive for $V_{dc}=48V$ and $T_I=0$

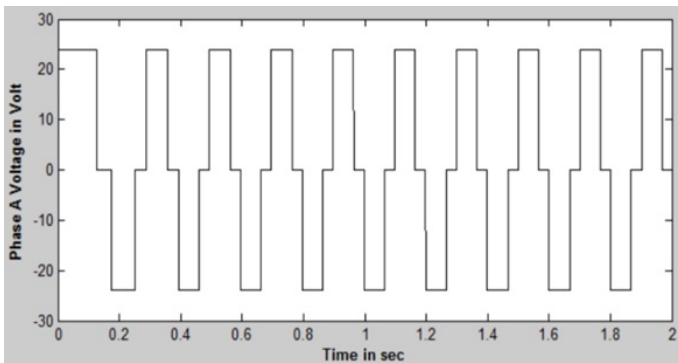


Figure 6: Phase-A Voltage vs. Time Response of a BLDC Motor drive for $V_{dc}=48V$ and Load torque (T_I)=0

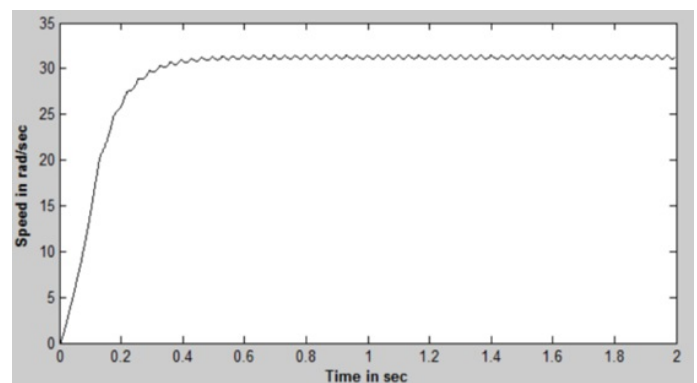


Figure 9: Speed vs Time response of a BLDC Motor drive for $V_{dc}=48V$ and $T_I=0$

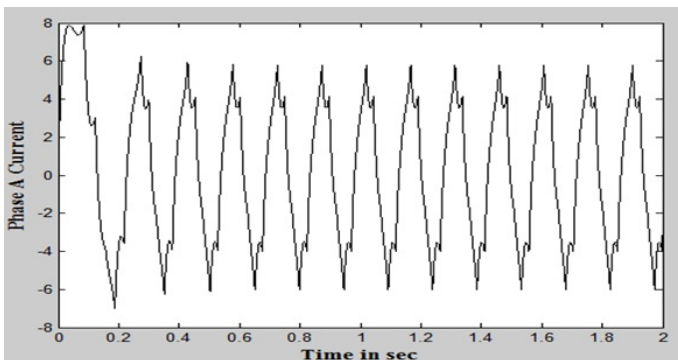


Figure 7: A-Phase Current vs. Time response of a BLDC Motor drive for $V_{dc}=48V$ and $T_I=0$

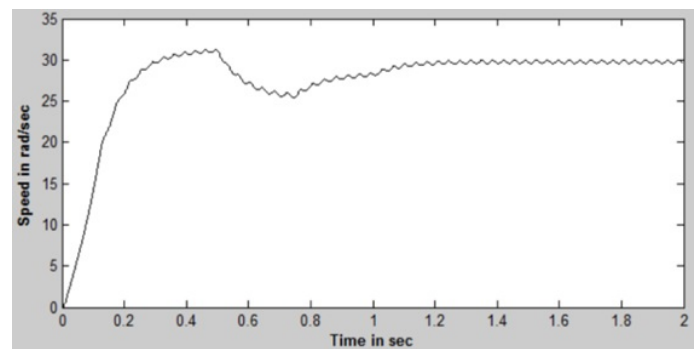


Figure 10: Speed vs Time response of a BLDC Motor drive for $V_{dc}=48V$ with $T_I=0$, $T_I=2$, $T_I=1$ & $T_I=0.5$

4. Simulation Results and Discussions

Different parameters of BLDC motor were simulated using MATLAB software for both no load and load condition and the simulation results—i.e. the nature of different responses—are discussed here. Fig. 6 and Fig. 7 represent the phase voltage and phase current vs time plot of an open-loop model of BLDC motor drive. In both load and no load condition the phase voltage and current plot are same. It means there is the effect of load on the voltage and current, as these are given from the supply end. The phase voltage response has an identified six step waveform in which there is a two-level VSI operating under 120-degree conduction mode in a bal-

ancing condition. The frequency of this waveform as well as phase current are found to gradually increase from the starting point because speed gradually builds up and is self-synchronized with the rotor position. It can be seen in Fig. 7 that the current waveform is not a pure sinusoid. The rotor position vs time is shown in Fig. 8. It starts from a negative position and goes up to the positive maximum position due to the change of position of a switching sequence of the six step VSI. The rotor position plot is also same for both conditions. Now the effect of load and no load can be judged from the next figure, i.e. from Fig. 9 and Fig. 10. These figures, i.e.

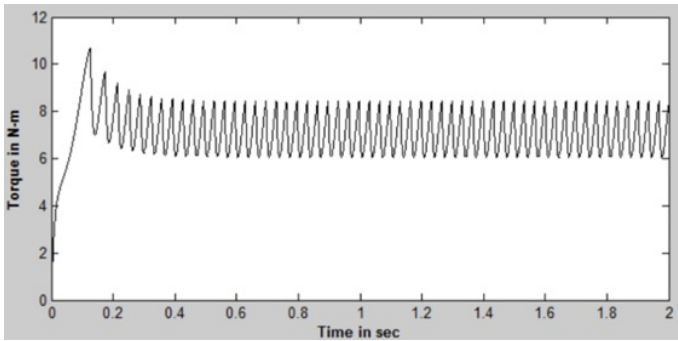


Figure 11: Electromagnetic Torque vs Time response of a BLDC Motor drive for $V_{dc}=48V$ and $T_I=0$

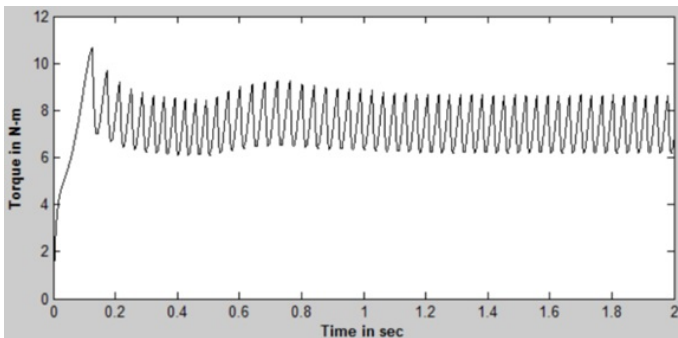


Figure 12: Electromagnetic Torque vs Time response of a BLDC Motor drive for $V_{dc}=48V$ with $T_I=0$, $T_I=2$, $T_I=1$ & $T_I=0.5$

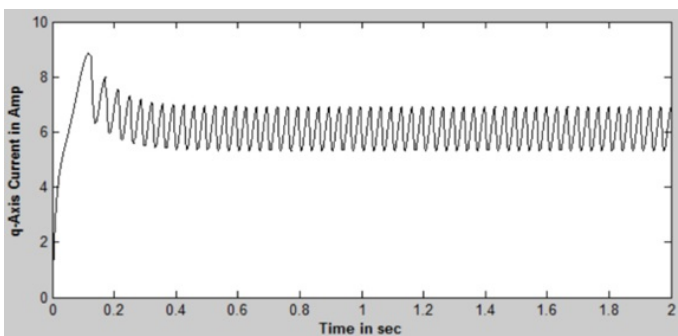


Figure 13: q-axis current vs. Time response of a BLDC Motor drive for $V_{dc}=48V$ and $T_I=0$

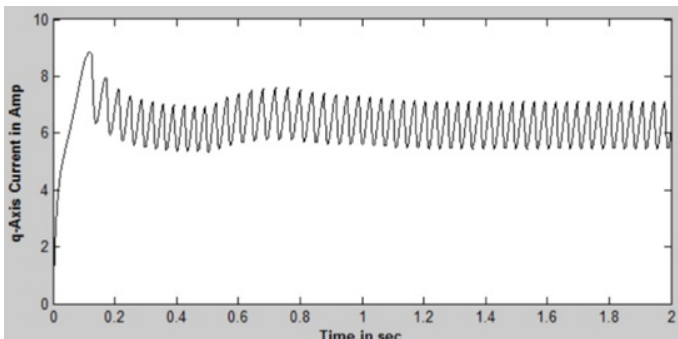


Figure 14: q-axis current vs Time response of a BLDC Motor drive for $V_{dc}=48V$ with $T_I=0$, $T_I=2$, $T_I=1$ & $T_I=0.5$

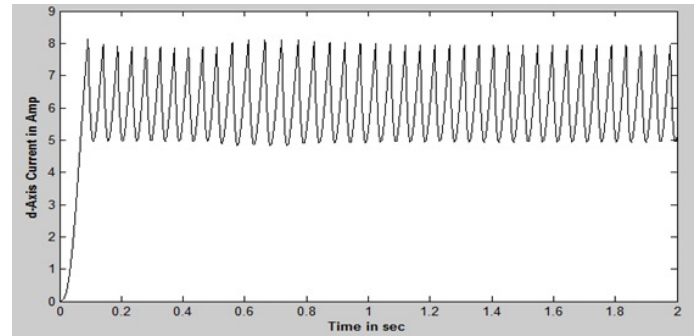


Figure 15: d-axis current vs Time response of a BLDC Motor drive for $V_{dc}=48V$ with $T_I=0$, $T_I=2$, $T_I=1$ & $T_I=0.5$

Fig. 9 and Fig. 10 represent the speed vs time response for input voltage 48 volt for no load and load condition respectively. It can be seen from Fig. 9 that the speed is increased from zero in transient condition and found to settle finally to a steady state value. The speed response has no tendency for instability at no load condition i.e. $T_L=0$. But from Fig. 10 we can say that with the application of load for a particular time period, the speed falls depending on the value of load applied to the motor and as the load is removed the motor achieves its steady state stable previous position. The important parameter is torque and so the electromagnetic torque vs time response to the same condition of the open loop model of BLDC motor drives is shown in Fig. 11 and Fig. 12 for no load and load accordingly. From this response, it can be seen that torque is initially higher for high current passing through the open loop model without connected to the load on the output side and finally reaches a steady state condition having some ripples. But, when the load is applied, the response showed an overshoot at that time. It means that with the increment of the load in the BLDC motor in an open loop configuration, the torque also increases as shown in Fig. 12. Actually, the electromagnetic torque of BLDC motor depends on the q-axis current and that we can find from Fig. 13 and Fig. 14, which are the plots of q-axis current for no load and load condition. The torque exactly follows the q-axis current response because this is the torque producing component of this model and so it has the same plot shape. It has been seen from Fig. 12 and Fig. 15, which are the plotting of the d axis current vs time characteristics, that the d-axis current is initially increased and finally settled at a steady state value with some ripples for both no load and load.

5. Conclusion

In this paper, a comparative performance study between No load and load condition of an open loop model of a Brushless DC (BLDC) Motor drive has been simulated in MATLAB based software. The different block of the open loop model of BLDC motor has also been discussed. The model is developed for a trapezoidal back EMF based BLDC motor, meaning the motor is operated through a three phase self-

synchronous 1200 conduction mode two level bridge voltage source inverter. This paper determines all the possible different responses of an open loop model of the BLDC motor drive under both load and no load condition and these responses are: speed response, rotor position, electromagnetic torque, phase voltages, phase currents, d-q axis currents. The inverter DC link voltage can be varied in order to achieve open loop speed control, which is similar to the armature voltage control of a separately excited conventional DC motor. This paper enriches the concept of the behavior of various components of a BLDC motor in an open loop load and no load condition.

6. References

- [1] P. Yedamale, Brushless DC (BLDC) Motor Fundamentals, Microship Technology Inc, 2003.
- [2] S. A. E. X. G. Santhosh Kumar, Brushless dc motor speed control using microcontroller, International Journal Of Current Engineering And Scientific Research (IJCESR) 2 (2015) 183–188.
- [3] K. T. Selvakumar P, Studies on bldc motor for position control using pid-fuzzy-neural network and anti-windup controllers, Australian Journal of Basic and Applied Sciences 1 (2013) 33–48.
- [4] J. V. Sreekala P, Application of neural network in speed control of brush-less dc motor using soft switching inverter, in: Proceedings of the IEEE International Conference on Engineering Education: Innovative Practices and Future Trends, 2012, p. 1–5.
- [5] R. S. N. A. R. Aris, A. S. A. G. A. Ghani, M. L. M. Zain, Enhancement of variable speed brushless dc motor using neural network, Indian Journal of Science and Technology 9 (14).
- [6] A. M. Ahmed, A. Ali-Eldin, M. S. Elksasy, F. F. Areed, Brushless dc motor speed control using both pi controller and fuzzy pi controller, International Journal of Computer Applications 109 (10) (2015) 29–35.
- [7] K. N. P. Yadav, R. Poola, High dynamic performance of a bldc motor with a front end converter using an fpga based controller for electric vehicle application, Turkish Journal of Electrical Engineering & Computer Sciences 24 (2016) 1636 – 1651.
- [8] T. Nag, S. B. Santra, A. Chatterjee, D. Chatterjee, A. K. Ganguli, Fuzzy logic-based loss minimisation scheme for brushless dc motor drive system, IET Power Electronics 9 (8) (2016) 1581–1589.
- [9] R. G. Balakrishna, P. Y. Reddy, Speed control of brushless dc motor using microcontroller, International Journal of Engineering Technology, Management and Applied Sciences 3 (2015) 11–26.
- [10] S. Hidayat, S. P. Hadi, Suharyanto, The design of the hybrid pid-anfis controller for speed control of brushless dc motor, Journal of Theoretical and Applied Information Technology 371 (2015) 367–375.
- [11] G. Paranjothi, R. Manikandan, Photovoltaic based brushless dc motor closed loop drive for electric vehicle, International Journal of Emerging Trends in Electrical and Electronics 10 (2014) 9–15.
- [12] I. V. Abramov, Y. R. Nikitin, A. I. Abramov, E. V. Sosnovich, P. Božek, Control and diagnostic model of brushless dc motor, Journal of Electrical Engineering 65 (5) (2014) 277–282.
- [13] H. Bayoumi, Ehab & Soliman, Pid/pi tuning for minimal overshoot of pm brushless dc motor drive using swarm optimization, Electromotion Scientific Journal 14 (2007) 198–208.
- [14] G. T. S. C. Sajeevan, T source inverter based permanent magnet brushless dc motor, International Journal of Science, Engineering and Technology Research (IJSETR) 4 (2015) 3437–3442.
- [15] R. S. S. Mittal, V. K. Gupta, Implementation and realization of brushless dc motor, International Journal of Scientific & Engineering Research 4 (2013) 913–918.
- [16] A. V. K. R. S. Patel, Modeling and performance analysis of pid controlled bldc motor and different schemes of pwm controlled bldc motor, International Journal of Scientific and Research Publications 3 (2013) 1–14.
- [17] H. WANG., Design and implementation of brushless dc motor drive and control system, in: International Workshop on Information and Electronics Engineering (IWIEE), Sci Verse ScienceDirect, ELSEVIER, Procedia Engineering 29, 2012, pp. 2219 – 2224.
- [18] C. P. Elangovan, Comparison analysis of different controllers for pwm inverter fed permanent magnet brushless dc motor, International Journal of Scientific Engineering and Research 3 (2012) 1–5.
- [19] S. Bharatkar, R. Yanamshetti, D. Chatterjee, A. Ganguli, Dual-mode switching technique for reduction of commutation torque ripple of brushless dc motor, IET electric power applications 5 (1) (2011) 193–202.
- [20] O. W. P. C. Krause, S. D. Sudhoff, Analysis of Electric Machinery and drives system, Wiley India Pvt. Ltd., 2014.
- [21] M. R. F. M. Ebadpour, M. B. B. Sharifian, A cost-effective position sensorless control for four-switch three-phase brushless dc motor drives using single current sensor, International Review of Automatic Control (I.R.E.A.CO.) 4 (2011) 386–393.
- [22] D. C. S. S. Bharatkar, Raju Yanamshetti, A. K. Ganguli, Reduction of commutation torque ripple in a brushless dc motor drive, in: 2nd IEEE International Conference on Power and Energy (PECon 08), no. 289 - 294, 2008.
- [23] M. Markovic, Y. Perriard, Simplified design methodology for a slotless brushless dc motor, IEEE trans. on Magnetics 42 (2006) 3842–3846.
- [24] F. C. F. Caricchi, F. G. Capponi, L. Solero, Experimental study on reducing cogging torque and no-load power loss in axial-flux permanent-magnet machines with slotted winding, IEEE Trans. On Industry Applications 40.
- [25] R. Krishnan, Electric Motor Drives: Modeling, Analysis and Control, Prentice Hall, 2001.
- [26] D. C. Hanselman, Effect of skew, pole count and slot count on brushless motor radial force, cogging torque and back emf, Proc. Inst. Elect. Eng., pt. B 144 (1997) 325–330.
- [27] P. Pillay, R. Krishnan, Modeling of permanent magnet motor drives, IEEE Trans. on Industrial Electronics 35 (1988) 537 – 554.
- [28] D. Hanselman, Brushless Permanent Magnet Motor Design, Mc. Graw Hill, 1994.
- [29] M. T. J. E., Brushless Permanent and Reluctance Motor Drives, Clarendon Press, Oxford, 1989.

Appendix

The parameters of the Brush-less DC motor (BLDC), on which the studies are made in this paper, are: Number of poles, $P = 4$, armature resistance, $r_s = 3.2$, D-axis synchronous inductance, $L_d = 0.0531\text{H}$, Q-axis synchronous inductance, $L_q = 0.041\text{H}$, rotor peak permanent flux linkage referred to the stator, $\phi_r = 0.418\text{Wb-turns}$, combined moment of inertia, $J = 0.061\text{kg-m}^2$.